Electronic Supplementary Information

Magnetic Anisotropy in Yb^{III} Complexes Candidates for Molecular Qubits: A Theoretical Analysis

Martín Amoza, Silvia Gómez-Coca and Eliseo Ruiz*

Departament de Química Inorgànica i Orgànica and Institut de Recerca de Química Teòrica i Computacional, Universitat de Barcelona,
Diagonal 645, 08028 Barcelona, Spain

email: eliseo.ruiz@qi.ub.es

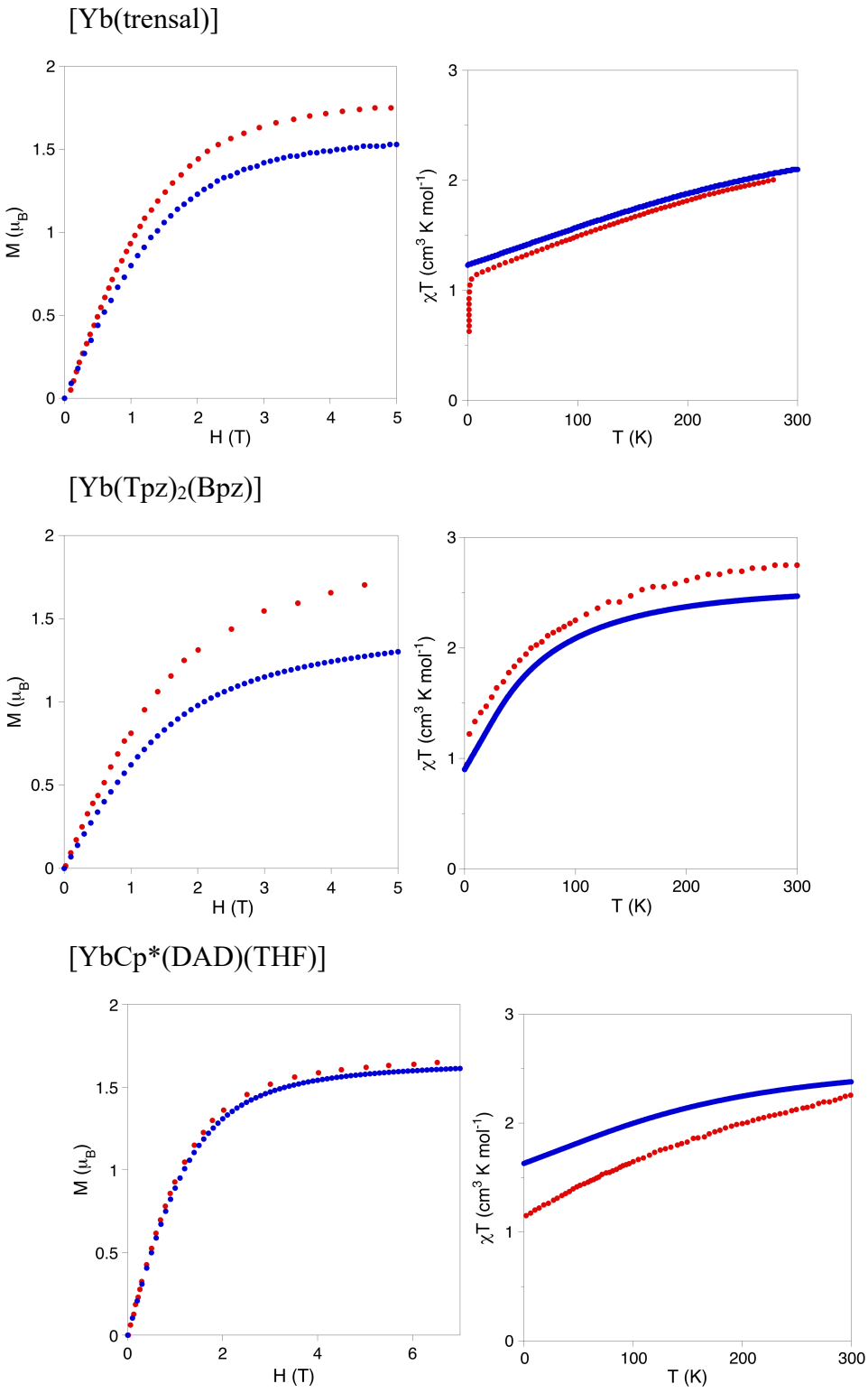

Figure S1. Experimental (red) and calculated (blue, CASPT2 level) magnetizations and susceptibilities for the three Yb^{III} complexes studied that are field-induced single-molecule magnets.

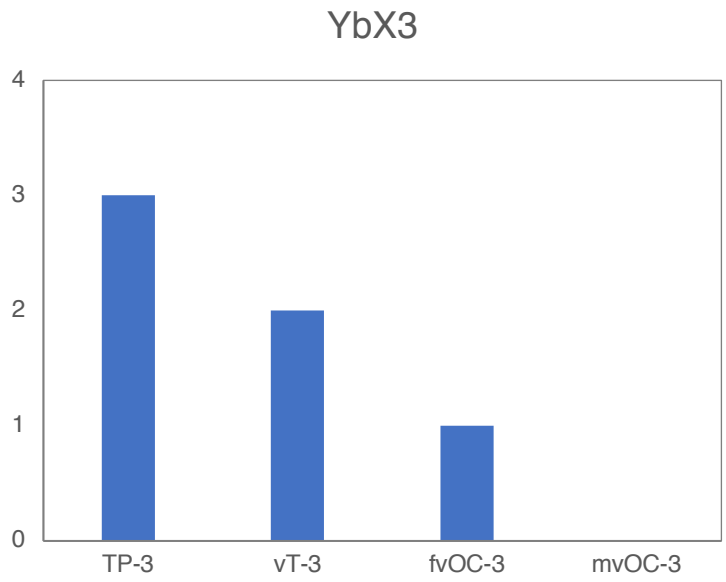

Figure S2. Number of hits for the different geometries with coordination number 3 of mononuclear Yb^{III} complexes found in CSD and classified with the Shape code.

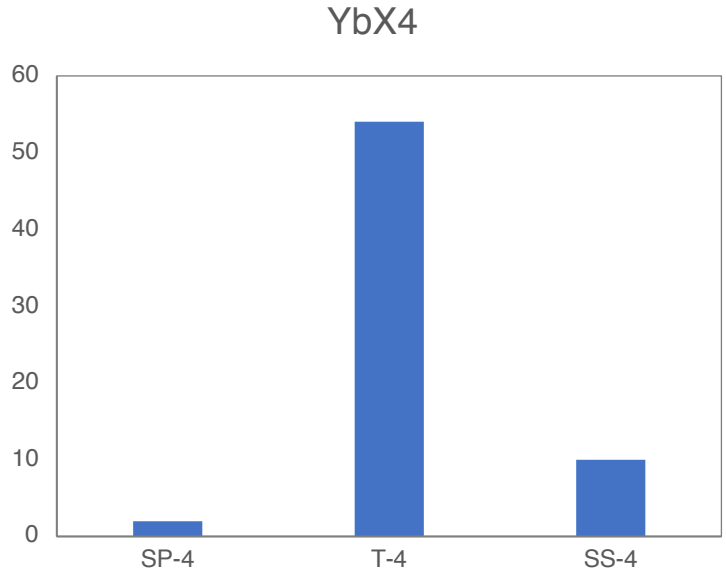

Figure S3. Number of hits for the different geometries with coordination number 4 of mononuclear Yb^{III} complexes found in CSD and classified with the Shape code.

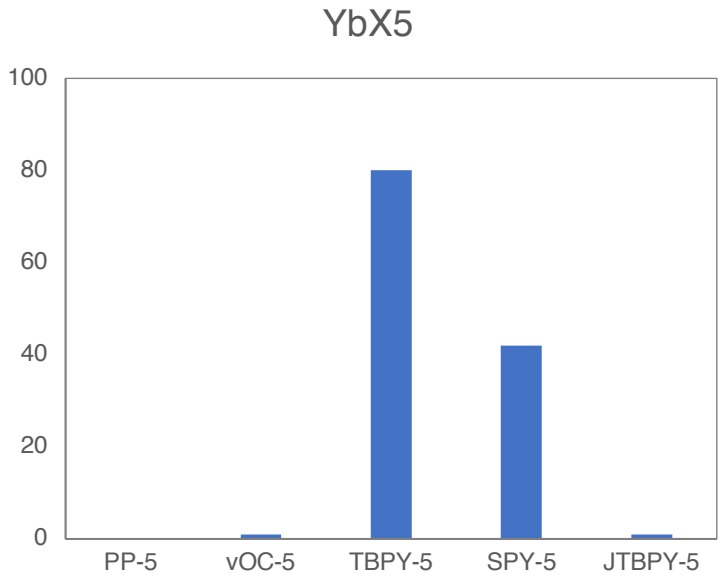

Figure S4. Number of hits for the different geometries with coordination number 5 of mononuclear Yb^{III} complexes found in CSD and classified with the Shape code.

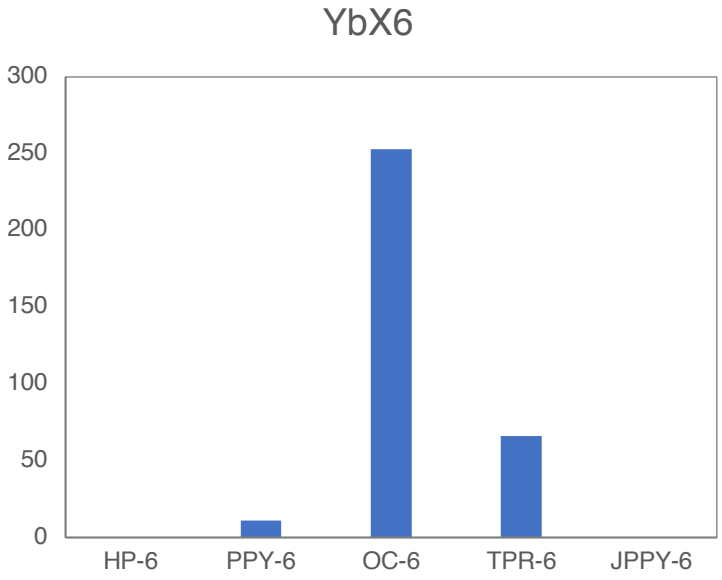

Figure S5. Number of hits for the different geometries with coordination number 6 of mononuclear Yb^{III} complexes found in CSD and classified with the Shape code.

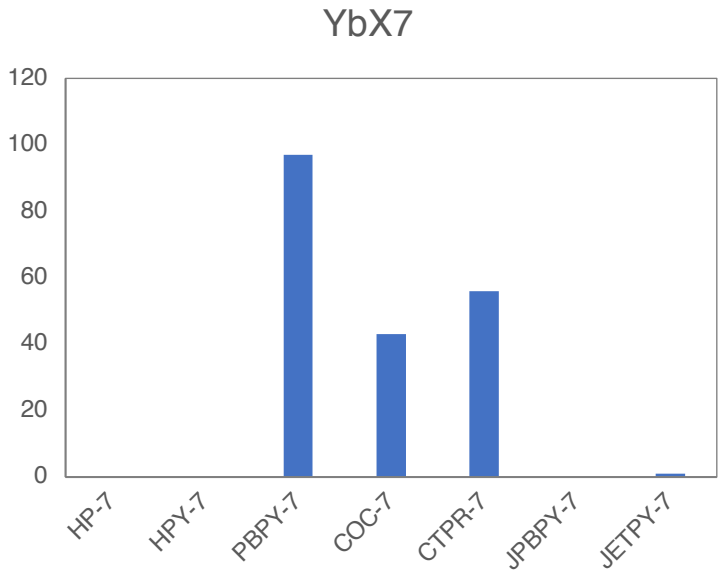

Figure S6. Number of hits for the different geometries with coordination number 7 of mononuclear Yb^{III} complexes found in CSD and classified with the Shape code.

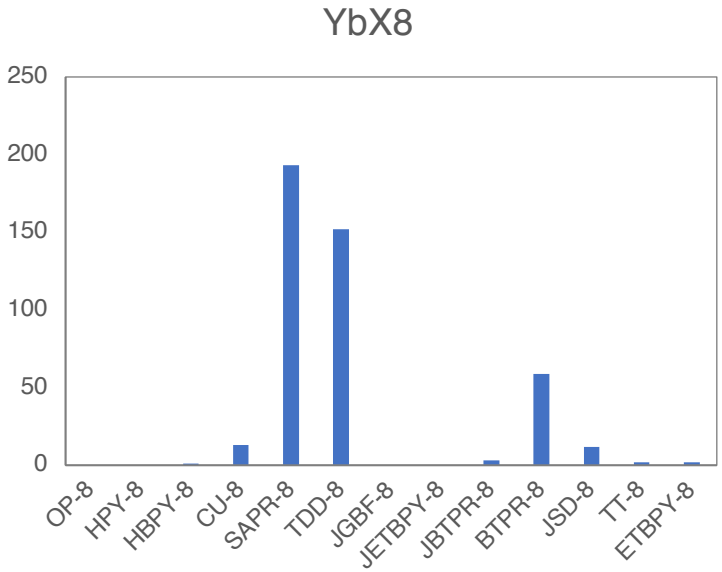

Figure S7. Number of hits for the different geometries with coordination number 8 of mononuclear Yb^{III} complexes found in CSD and classified with the Shape code.

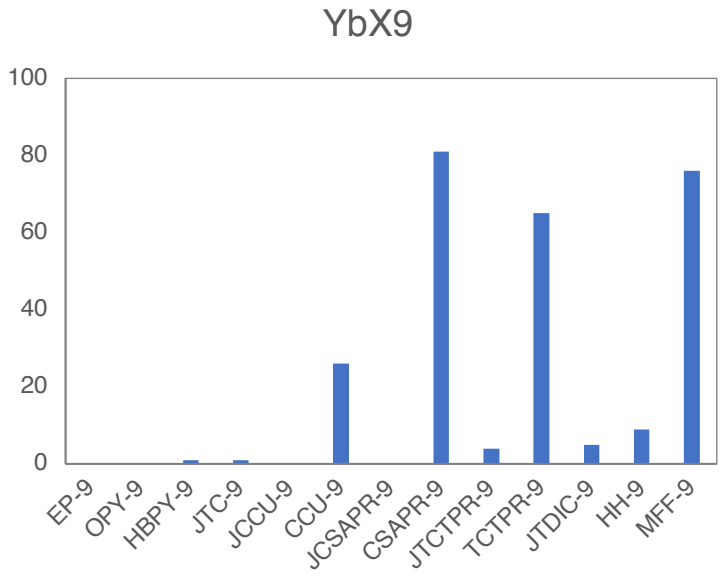

Figure S8. Number of hits for the different geometries with coordination number 9 of mononuclear Yb^{III} complexes found in CSD and classified with the Shape code.

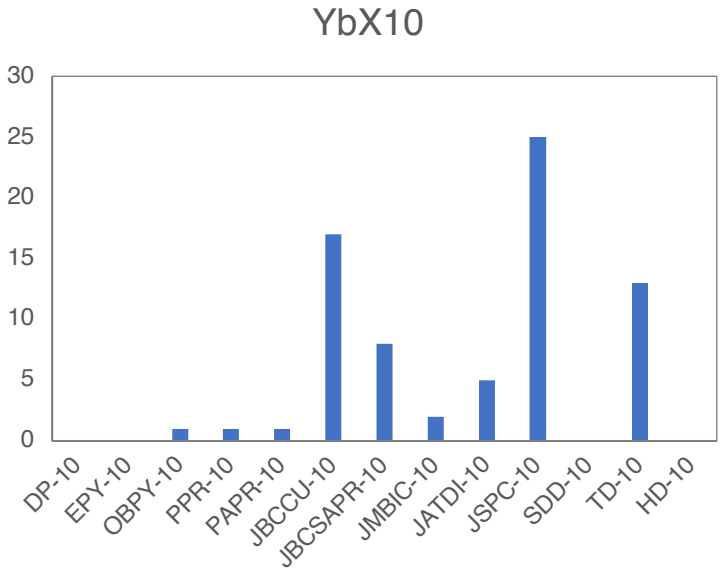

Figure S9. Number of hits for the different geometries with coordination number 10 of mononuclear Yb^{III} complexes found in CSD and classified with the Shape code.

Table S1. CASPT2/RASSI results for the $[Yb(H_2O)_n]^{3+}$ models. The values of the different components of the g-tensor and the percentage of the state M_J = 7/2 of the fundamental state are shown, as well as the values obtained for the relaxation of the magnetization through the tunnel effect in the ground state (state 0) and Orbach through the first excited state (state 1). Matrix elements of the transition magnetic moments between two states above 0.10 indicate that the relaxation path is relevant.

model	label	$g_\perp$	$g_\parallel$	M_J 7/2 (%)	Tunnel state 0	Orbach state 1
Linear-2	2_1	6.51	1.17	0	1.52	0.06
Divacant Tetrahedron-2	2_2	0.56	7.38	88	0.13	0.87
Trigonal Planar-3	3_1	0.42	7.96	100	0.10	0.12
Square Planar-4	4_1	0.07	7.92	99	0.01	0.02
Tetrahedron-4	4_2	3.20	5.53	66	0.75	0.98
Trigonal Bipyramid-5	5_1	3.36	5.82	69	0.71	1.07
Square Pyramid-5	5_2	0.18	7.84	98	0.04	0.08
Octahedron-6	6_1	2.21	4.89	65	0.51	1.00
Trigonal Prism-6	6_2	0.74	7.56	96	0.16	0.82
Capped Trigonal Prism-7	7_2	0.30	7.53	91	0.06	0.72
Pentagonal Bipyramid-7	7_3	0.14	7.97	100	0.03	0.17
Square Antiprism -8	8_1	0.10	7.84	97	0.02	0.09
Triangular Dodecahedron-8	8_2	2.62	5.88	67	0.53	0.80
Capped Square Antiprism-9	9_1	1.35	6.27	83	0.30	0.54
Tricapped Trigonal Prism-9	9_2	1.06	6.24	73	0.24	1.16
Sphenocorona-10	10_1	2.04	7.11	90	0.47	0.65

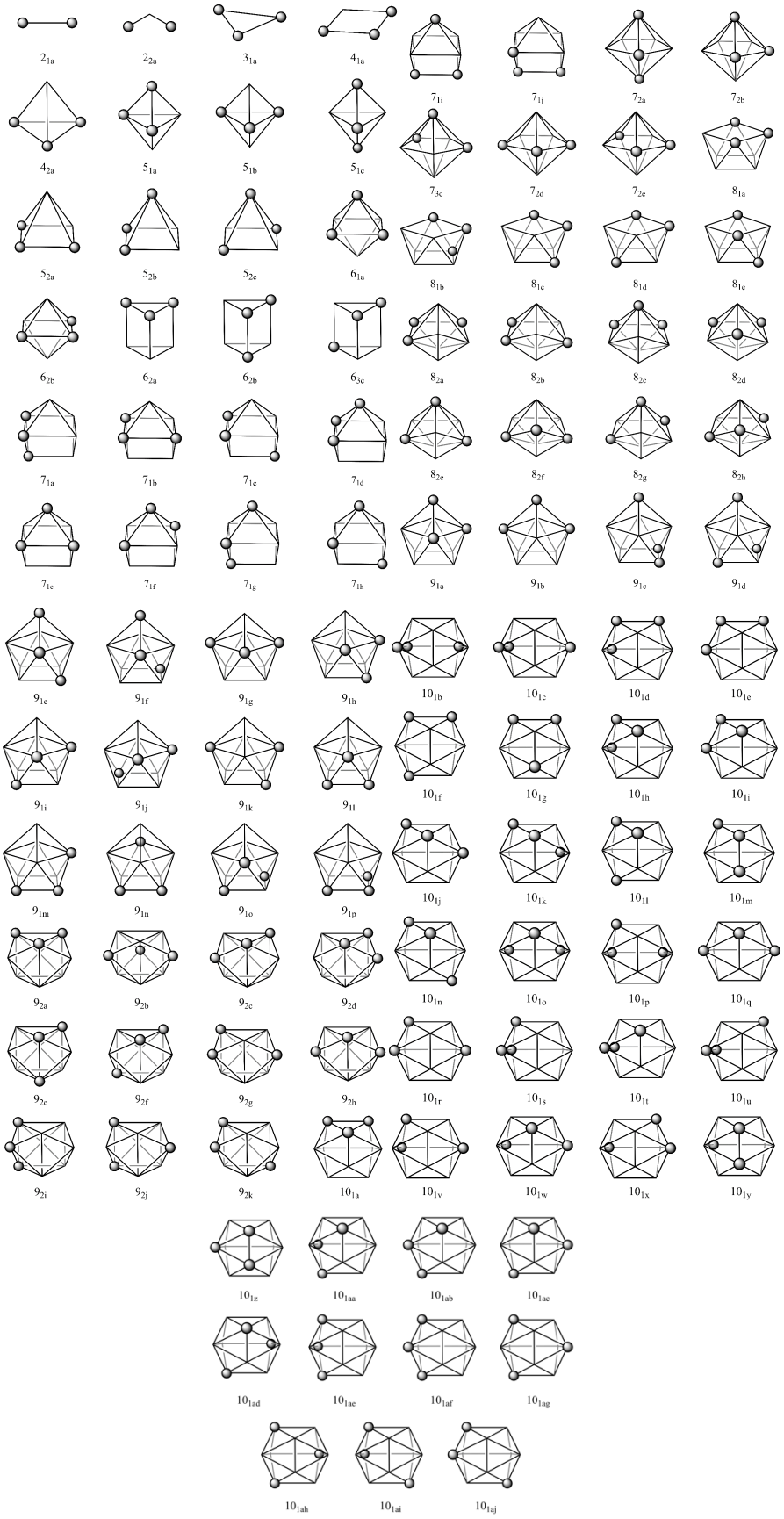

Figure S10. Calculated $[Yb(OH)_3(H_2O)_{n-3}]$ models at CASPT2/RASSI level (see Tables S2, S3 and S4). The hydroxo ligands are represented with the gray spheres in the geometry.

Table S2. Results for the neutral models of coordination from 2 to 7 with OH^- and H_2O ligand, $[Yb(OH)_3(H_2O)_{n-3}]$ (see labels Fig. S10). The values of the different components of the g-tensor and the percentage of the state $M_J = 7/2$ of the fundamental state are shown, as well as the values obtained for the relaxation of the magnetization through the tunnel effect in the ground state (state 0) and the first excited state (state 1) and Orbach through the first excited state (state 1). Matrix elements of the transition magnetic moments between two states above 0.10 indicate relevant mechanism. Systems with spin relaxation though excited states in bold. In red, systems with intermediate g_{zz} value.

Model	label	g_{xx}	g_{yy}	g_{zz}	M_J 7/2 (%)	Tunnel state 0	Orbach state 1	Tunnel state 1
Linear-2	**1a**	**1.11**	**3.27**	**5.77**	**68**	**0.73**	**1.08**	**0.41**
Divacant tetrahedron-2	2a	0.98	2.64	6.24	74	0.60	1.06	0.62
Trigonal Planar-3	**1a**	**0.15**	**0.16**	**7.98**	**100**	**0.05**	**0.06**	**0.07**
Plano Cuadrado-4	**1a**	**0.16**	**0.25**	**7.88**	**98**	**0.07**	**0.11**	**0.71**
Tetrahedron-4	**2a**	**0.25**	**0.28**	**7.91**	**99**	**0.09**	**0.12**	**0.10**
	1a	**0.23**	**0.34**	**7.86**	**98**	**0.10**	**0.23**	**1.03**
Trigonal Bipyramid-5	**1b**	**0.18**	**0.19**	**7.97**	**100**	**0.06**	**0.09**	**0.18**
	1c	0.60	1.14	7.38	90	0.29	0.44	1.02
	2a	0.37	0.60	7.72	96	0.16	0.32	1.06
Square Pyramid-5	**2b**	**0.16**	**0.30**	**7.82**	**98**	**0.08**	**0.24**	**0.50**
	2c	0.63	1.36	7.15	87	0.33	0.91	0.88
Octahedron-6	**1a**	**0.29**	**2.32**	**5.61**	**70**	**0.44**	**0.94**	**0.47**
	1b	0.35	0.67	7.61	94	0.17	0.71	1.01
	2a	**0.22**	**1.91**	**5.71**	**65**	**0.36**	**1.27**	**0.60**
Trigonal Prism-6	2b	0.50	0.89	7.57	94	0.23	1.03	1.02
	2c	**0.22**	**0.38**	**7.54**	**91**	**0.10**	**0.86**	**1.33**
	1a	0.64	0.69	6.87	79	0.22	0.79	1.53
	1b	0.88	2.24	6.60	81	0.52	0.62	1.19
	1c	0.61	1.58	6.90	83	0.37	1.05	1.02
	1d	0.35	0.60	7.14	84	0.16	0.72	1.60
Capped Trigonal Prism-7	**1e**	**0.04**	**0.08**	**7.72**	**95**	**0.02**	**0.14**	**0.12**
	1f	**0.25**	**0.37**	**7.83**	**98**	**0.10**	**0.19**	**0.75**
	1g	0.37	0.62	7.65	94	0.16	0.34	0.91
	1h	**0.23**	**0.34**	**7.71**	**95**	**0.10**	**0.27**	**0.86**
	1i	**0.05**	**0.09**	**7.73**	**95**	**0.02**	**1.06**	**0.52**
	1j	**0.17**	**0.19**	**7.92**	**99**	**0.06**	**0.16**	**0.52**
	2a	0.79	1.67	7.09	88	0.41	0.92	1.02
	2b	**0.07**	**0.21**	**7.65**	**94**	**0.05**	**0.76**	**0.09**
Pentagonal Bipyramid-7	2c	0.63	1.42	7.16	89	0.34	1.02	0.72
	2d	0.33	0.47	7.84	98	0.13	0.78	1.27
	2e	**0.24**	**0.36**	**7.81**	**97**	**0.10**	**0.74**	**0.94**

Table S3. Results for the neutral models of coordination 8 and 9, $[Yb(OH)_3(H_2O)_{n-3}]$ (see labels Fig. S10). The values of the different components of the g-tensor and the percentage of the state $M_J = 7/2$ of the fundamental state are shown, as well as the values obtained for the relaxation of the magnetization through the tunnel effect in the fundamental state (state 0) and the first excited state (state 1) and Orbach through the first excited state (state 1). Matrix elements of the transition magnetic moments between two states above 0.10 indicate relevant mechanism. Systems with spin relaxation though excited states in bold. In red, systems with intermediate g_{zz} value.

Model	label	g_{xx}	g_{yy}	g_{zz}	M_J 7/2 (%)	Tunnel state 0	Orbach state 1	Tunnel state 1
Square Antiprism-8	**1a**	**0.20**	**0.24**	**7.87**	**98**	**0.07**	**0.56**	**0.85**
	1b	**0.14**	**0.25**	**7.60**	**93**	**0.06**	**0.13**	**0.35**
	1c	**0.23**	**0.36**	**7.77**	**96**	**0.10**	**0.20**	**0.82**
	1d	**0.13**	**0.20**	**7.72**	**94**	**0.06**	**0.09**	**0.63**
	1e	0.34	0.63	7.60	93	0.16	0.80	0.90
Triangular Dodecahedron-8	2a	0.47	0.72	7.68	96	0.20	0.35	0.86
	2b	**0.15**	**0.22**	**7.75**	**95**	**0.06**	**0.11**	**0.78**
	2c	0.27	1.16	6.50	78	0.24	0.92	0.80
	2d	0.27	0.50	7.71	95	0.13	0.77	0.77
	2e	0.35	0.73	7.33	88	0.18	0.38	0.96
	2f	**0.07**	**0.15**	**7.84**	**97**	**0.04**	**0.06**	**0.57**
	2g	1.06	2.83	6.17	76	0.65	1.04	0.65
	2h	0.34	0.66	7.54	92	0.17	0.47	0.96
Capped Square Antiprism-9	1a	0.87	1.47	7.18	91	0.39	0.61	0.59
	1b	0.32	0.58	7.66	95	0.15	1.03	0.47
	1c	**0.16**	**0.36**	**7.65**	**94**	**0.09**	**0.90**	**1.51**
	1d	0.43	0.53	7.87	99	0.16	0.20	0.29
	1e	**0.07**	**0.18**	**7.82**	**98**	**0.04**	**0.15**	**0.66**
	1f	0.41	0.75	7.55	92	0.19	0.74	1.03
	1g	0.64	1.10	7.51	94	0.29	0.67	1.00
	1h	0.37	0.77	7.36	91	0.19	0.39	0.50
	1i	0.52	0.79	7.68	96	0.22	0.82	1.38
	1j	0.31	0.53	7.67	94	0.14	0.25	0.90
	1k	0.29	0.48	7.50	91	0.13	0.92	1.07
	1l	4.95	3.21	0.80	1	1.36	1.37	1.46
	1m	**0.13**	**0.20**	**7.85**	**98**	**0.06**	**0.12**	**0.43**
	1n	0.43	0.87	7.25	86	0.22	0.90	0.91
	1o	1.12	2.96	6.06	77	0.68	1.06	0.58
	1p	**0.22**	**0.39**	**7.76**	**98**	**0.10**	**0.26**	**0.45**
	2a	**1.60**	**2.48**	**5.30**	**68**	**0.68**	**1.03**	**0.63**
	2b	0.62	0.66	7.84	99	0.21	0.25	0.38
	2c	**0.20**	**0.26**	**7.84**	**98**	**0.08**	**0.13**	**0.79**
	2d	**0.59**	**2.69**	**5.80**	**93**	**0.55**	**0.97**	**0.63**
	2e	0.67	1.02	7.58	96	0.28	0.46	0.84
Tricapped Trigonal Prism-9	2f	0.37	0.66	7.43	94	0.17	0.86	1.12
	2g	0.62	1.32	7.15	93	0.32	0.96	0.96
	2h	0.43	0.60	7.72	96	0.17	0.70	1.52
	2i	0.65	0.73	7.67	95	0.23	0.38	0.45
	2j	0.37	0.48	7.86	78	0.14	0.18	0.17
	2k	0.65	1.43	7.15	95	0.35	1.02	1.00

Table S4. Results for the neutral models of coordination 10 with OH^- and H_2O ligand, $[Yb(OH)_3(H_2O)_7]$ (see labels Fig. S10). The values of the different components of the g-tensor and the percentage of the state $M_J = 7/2$ of the fundamental state are shown, as well as the values obtained for the relaxation of the magnetization through the tunnel effect in the fundamental state (state 0) and the first excited state (state 1) and Orbach through the first excited state (state 1). Matrix elements of the transition magnetic moments between two states above 0.10 indicate relevant mechanism. Systems with spin relaxation though excited states in bold.

Model	label	g_{xx}	g_{yy}	g_{zz}	M_J 7/2 (%)	Tunnel state 0	Orbach state 1	Tunnel state 1
Sphenocorona-10	1a	0.84	1.82	6.96	86	0.44	0.77	0.82
	1b	0.54	1.08	7.35	90	0.27	0.79	0.76
	1c	0.46	0.86	7.31	87	0.22	0.77	0.60
	1d	0.85	1.23	7.45	94	0.35	0.46	0.34
	1e	0.70	0.87	7.69	97	0.26	0.31	0.29
	1f	0.84	1.70	7.10	88	0.42	0.92	0.89
	1g	0.45	0.75	7.44	91	0.20	0.72	1.51
	1h	0.35	0.41	7.80	98	0.13	0.24	0.22
	1i	1.06	1.46	7.25	94	0.42	0.91	0.38
	1j	0.54	0.74	7.72	97	0.21	0.31	0.23
	1k	**0.10**	**0.36**	**6.86**	**82**	**0.08**	**0.78**	**1.33**
	1l	0.77	1.79	6.91	85	0.43	0.89	0.93
	1m	0.45	0.79	7.47	92	0.21	0.57	1.57
	1n	0.87	2.00	6.78	82	0.48	0.88	1.46
	1o	0.23	0.46	7.50	91	0.11	0.31	0.44
	1p	5.00	3.66	1.14	3	1.44	1.07	0.41
	1q	0.34	0.52	7.74	96	0.14	1.02	0.21
	1r	0.82	1.32	7.42	94	0.36	0.87	0.84
	1s	1.09	1.96	6.79	88	0.51	0.59	0.45
	1t	0.49	0.74	7.68	96	0.21	0.40	0.85
	1u	0.87	1.86	6.70	81	0.46	0.82	0.71
	1v	0.84	1.42	7.33	92	0.38	0.92	1.38
	1w	0.65	1.28	7.16	86	0.32	0.72	1.43
	1x	0.84	1.25	7.47	94	0.35	0.88	0.98
	1y	0.30	0.55	7.55	93	0.14	0.41	0.97
	1z	1.13	1.33	6.89	89	0.41	0.85	1.30
	1aa	0.67	1.19	7.08	87	0.31	0.83	0.98
	1ab	0.35	0.53	7.69	96	0.15	1.00	0.56
	1ac	0.63	1.13	7.41	93	0.29	0.57	0.76
	1ad	0.42	0.56	7.82	98	0.16	0.23	0.75
	1ae	0.67	1.03	7.54	95	0.28	0.44	0.44
	1af	0.68	0.86	7.69	97	0.26	0.28	0.51
	1ag	0.72	0.82	7.75	98	0.26	0.28	0.24
	1ah	0.77	1.24	7.41	93	0.34	0.57	0.87
	1ai	0.93	1.84	7.01	87	0.46	0.99	1.21
	1aj	0.78	1.36	7.35	92	0.36	0.90	1.43

Acronyms of Table 1

DBP 2,6-di-t-butil-phenoxide

Hna 1-Naphthoic acid

Hpyzc Pyrazinoic ac

H_3Trensal 2,2‘,2‘ ‘-Tris(salicylideneimino)triethylamine

BcrCOO (μ_6-C_6H_5)$Cr(CO)_3$

tta 2-thenoyltrifluoroacetonateanion

L^1 4,5-bis(thiomethyl)-40-carboxylictetrathiafulvalene

L^2 4,5-bis(thiomethyl)-40-ortho-pyridyl-N-oxide-carbamoyl-tetrathiafulvalene

H_2L^3 N,N′-bis(2-oxy-3-methoxybenzylidene)-1,2-phenylenediamine

L^4 N,N′- bis(pyridin-2-ylmethylene)ethane-1,2-diamine

DBM dibenzoylmethanide

Tpz hydrotris(pyrazolyl)borate

Bpz dihydrobis(pyrazolyl)borate

Dnbz 3,5-dinitrobenzoate

DAD $[2,6\text{-}Me_2C_6H_3NCH{=}CHNC_6H_3Me_2\text{-}2,6]^{2-}$

H-2-FBz 2-fluorobenzoic acid

2-qpH_2 2-Quinolinephosphonic acid

apdo 4,4’-azopyridine-1,1’-dioxide

terpy 2,2’6’,2”-terpyridine

tmh 2,2,6,6-tetramethylheptanoate

HAT 1,4,5,8,9,12-hexaazatriphenylene

PyrCOO Pyrazinoic acid

teaH_3 Triethanolamine

Piv Trimethylacetate

HL^5 2-(2′-hydroxy-3′-methyloxy-phenyl)- benzimidazole

HL^6 3-methoxysalicylaldehyde

H_2L^7 4,5-bis(carboxylic)-4’,5’-methyldithiotetrathiafulvene

HL^8 2-(tetrazol-5-yl)-1,10-phenanthroline

HAC 9-anthrancenecarboxylic acid

H_2L^9 N,N’-dimethyl-N,N’-bis(2-hydroxy-3-formyl-5-bromobenzyl)ethylenediamine

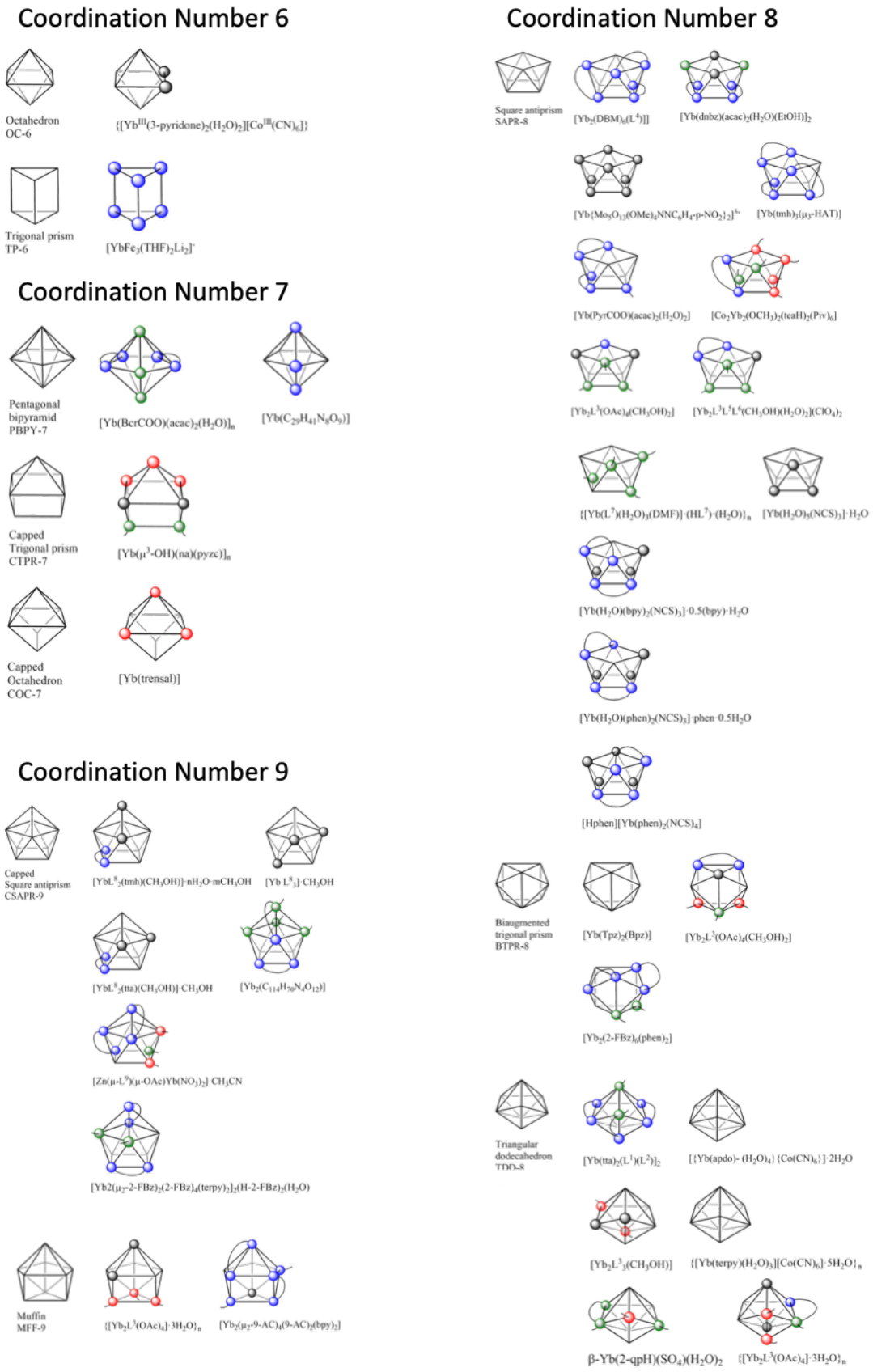

Figure S11. Charge distribution of ligands in the Yb^{III} complexes found in the literature indicated in Table 1. The vertices indicate the position of a ligand giving ligand: (empty vertex) no charge; (gray sphere) charge 1-; (red sphere) charge 1- shared between centers; (blue sphere) charge 1- delocalized without sharing between centers; (green sphere) charge 1- delocalized shared between centers.